
Large-scale Optimal Transport

Weijie Chen*
School of Physics
Peking University
1500011335
1500011335@pku.edu.cn

Dinghuai Zhang
School of Mathematics
Peking University
1600013525
1600013525@pku.edu.cn

1 Introduction to Optimal Transport

Optimal transport (OT) problems are an important series of problems considering the minimal cost of transportation, receiving increasing attention from the community of applied mathematics. Its history can be date back to 18th century, the time of the French engineer Gaspard Monge or 1920s when mathematicians were trying to figure out a way to move things efficiently during World War I. Sometimes optimal transport can be seen as some kind of network flow problem, aiming to "transport" one distribution μ to another distribution ν under some certain conditions², see figure 1. To put it in another way, given two distributions and a cost function, we aim to find a transport method that minimize a certain kind of cost. A specific definition can be seen in 1 and 4.

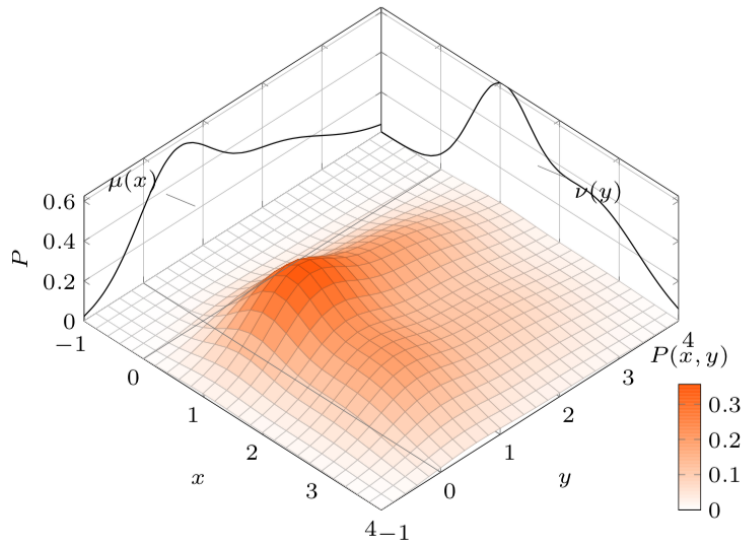


Figure 1: an example of optimal transport

*Pre-admission 2019 PKU AAIS

²figure is taken from Justin Solomon's tutorial

Over nearly 200 years, theory of optimal transport have not made much progress until some big mathematical breakthroughs in the 1980s and 1990s. Since then the field has flourished and optimal transport theory has found applications in PDEs, geometry, statistics, economics and image processing [5]. However, although it is such a prosperous research field, efficient algorithm to numerically solve continuous or discrete optimal transport problems is absent. While there are some existing algorithms [6] [7], there is still vast space for improvement.

In this report, we derive and implement some algorithms for solving a discrete optimal transport problem from a linear programming view. For some of them which is hard for tuning, we make some discussion about the reasons. Furthermore, we dive into the deep reasons for the good or bad performance of some algorithms. Our codes can be reached in GitHub: <https://github.com/zdhNarsil/OptimalTransport> or <https://github.com/BaozCWJ/OptimalTransport>.

2 Problem Statement

The standard formulation of optimal transport are derived from couplings. [8] That is, let (\mathcal{X}, μ) and (\mathcal{Y}, ν) be two probability spaces, and a probability distribution π on $\mathcal{X} \times \mathcal{Y}$ is called *coupling* if $proj_{\mathcal{X}}(\pi) = \mu$ and $proj_{\mathcal{Y}}(\pi) = \nu$. An optimal transport between (\mathcal{X}, μ) and (\mathcal{Y}, ν) , or an optimal coupling, is a coupling minimize

$$\int_{\mathcal{X} \times \mathcal{Y}} c(x, y) d\pi(x, y) \quad (1)$$

Optimal transport problems can be categorized according to the discreteness of μ and ν . In this report, we only consider discrete optimal transport problems, where the two distributions are distributions of finite weighted points. A discrete optimal transport problem can be formulated into a linear program as

$$\begin{aligned} \min_{\pi} \quad & \sum_{i=1}^m \sum_{j=1}^n c_{ij} \pi_{ij} \\ s.t. \quad & \sum_{j=1}^n \pi_{ij} = \mu_i, \forall i \\ & \sum_{i=1}^m \pi_{ij} = \nu_j, \forall j \\ & \pi_{ij} \geq 0, \end{aligned} \quad (2)$$

where c stands for the cost and s for the transportation plan, while μ and ν are restrictions. Note that we always suppose $c \geq 0$, $\mu \geq 0$, $\nu \geq 0$ and $\sum_{i=1}^m \mu_i = \sum_{j=1}^n \nu_j = 1$ implicitly. From realistic background, c is always valued the squared Euclidean distanced or some other norms. Note that there are mn variables in this formulation, and this leads to intensive computation.

In order to decrease the number of variables, we can derive the dual problem of discrete optimal transport.

$$\begin{aligned} \max_{\lambda, \eta} \quad & \sum_{i=1}^m \mu_i \lambda_i + \sum_{j=1}^n \nu_j \eta_j \\ \text{s.t.} \quad & c_{ij} - \lambda_i - \eta_j \geq 0, \forall i, j \end{aligned} \quad (3)$$

Although this formulation only has $m + n$ variables, there are still challenges including the recovery of π from λ and η and the great number of constraints.

3 Algorithms

3.1 ADMM for Primal Problem

We first implement a first order algorithm called **alternative direction method of multipliers** (ADMM). According to a reformulation of primal problem,

$$\begin{aligned} \min_{\pi} \quad & \sum_{i=1}^m \sum_{j=1}^n c_{ij} \pi_{ij} + \mathbb{I}_+(\hat{\pi}) \\ \text{s.t.} \quad & \sum_{j=1}^n \pi_{ij} = \mu_i, \forall i \\ & \sum_{i=1}^m \pi_{ij} = \nu_j, \forall j \\ & \pi = \hat{\pi} \end{aligned} \quad (4)$$

where \mathbb{I}_+ is indicator of $\mathbb{R}_+^{m \times n}$. The augmented Lagrangian can be written as

$$\begin{aligned} \mathcal{L}_\rho(\pi, \hat{\pi}, \lambda, \eta, e) = & \sum_{i=1}^m \sum_{j=1}^n c_{ij} \pi_{ij} + \mathbb{I}_+(\hat{\pi}) \\ & + \sum_{i=1}^m \lambda_i \left(\mu_i - \sum_{j=1}^n \pi_{ij} \right) + \sum_{j=1}^n \eta_j \left(\nu_j - \sum_{i=1}^m \pi_{ij} \right) + \sum_{i=1}^m \sum_{j=1}^n e_{ij} (\pi_{ij} - \hat{\pi}_{ij}) \\ & + \frac{\rho}{2} \sum_{i=1}^m \left(\mu_i - \sum_{j=1}^n \pi_{ij} \right)^2 + \frac{\rho}{2} \sum_{j=1}^n \left(\nu_j - \sum_{i=1}^m \pi_{ij} \right)^2 + \frac{\rho}{2} \sum_{i=1}^m \sum_{j=1}^n (\pi_{ij} - \hat{\pi}_{ij})^2 \end{aligned} \quad (5)$$

The minimizer of $\hat{\pi}$ can be written easily as

$$\operatorname{argmin}_{\hat{\pi}} \mathcal{L}_\rho(\pi, \hat{\pi}, \lambda, \eta, e) = \max \left(\pi + \frac{e}{\rho}, 0 \right) \quad (6)$$

For the minimizer of π , we can derive the following equation:

$$\sum_{k=1}^n \pi_{ik} + \sum_{k=1}^m \pi_{kj} + \pi_{ij} = \frac{1}{\rho} (-e_{ij} + \lambda_i + \eta_j - c_{ij}) + \mu_i + \nu_j + \hat{\pi}_{ij} \equiv r_{ij} \quad (7)$$

It's a linear equation of π_{ij} for the given r_{ij} , which can be solved directly.

$$\pi_{ij} = r_{ij} - \frac{1}{n+1} \sum_{k=1}^n \left(r_{ik} - \frac{1}{m+n+1} \sum_{l=1}^m r_{lk} \right) - \frac{1}{m+1} \sum_{k=1}^m \left(r_{kj} - \frac{1}{m+n+1} \sum_{l=1}^n r_{kl} \right) \quad (8)$$

Then, we can write the explicit form of ADMM algorithm. This algorithm is implemented in **ADMM_primal.py**.

Algorithm 1: Alternating direction method of multipliers for the primal problem

Input: input data c, μ, ν , step size α , penalty scalar ρ and maximum iteration N

Output: solution π

```

1 initializing  $k = 0$ 
2  $\pi^{(k)}, \hat{\pi}^{(k)}, e^{(k)}, \lambda^{(k)}, \eta^{(k)} := 0$ 
3 while  $k < N$  do
4    $\pi^{(k+1)} := \operatorname{argmin}_{\pi} \mathcal{L}_{\rho}(\pi, \hat{\pi}^{(k)}, \lambda^{(k)}, \eta^{(k)}, e^{(k)})$ 
5    $\hat{\pi}^{(k+1)} := \operatorname{argmin}_{\hat{\pi}} \mathcal{L}_{\rho}(\pi^{(k+1)}, \hat{\pi}, \lambda^{(k)}, \eta^{(k)}, e^{(k)})$ 
6    $\lambda^{(k+1)} := \lambda^{(k)} + \alpha\rho(\mu - \sum_{j=1}^n \pi_{ij})$ 
7    $\eta^{(k+1)} := \eta^{(k)} + \alpha\rho(\nu - \sum_{i=1}^m \pi_{ij})$ 
8    $e^{(k+1)} := e^{(k)} + \alpha\rho(\pi - \hat{\pi})$ 
9    $k := k + 1$ 
10 end
11 return  $\hat{\pi}$ 

```

3.2 ADMM for Dual Problem

According the reformulation of dual problem,

$$\begin{aligned} \min_{\lambda, \eta} \quad & - \sum_{i=1}^m \mu_i \lambda_i - \sum_{j=1}^n \nu_j \eta_j + \mathbb{I}_+(e) \\ \text{s.t.} \quad & c_{ij} - \lambda_i - \eta_j - e_{ij} = 0, \forall i, j \end{aligned} \quad (9)$$

we can write down the augmented Lagrangian as

$$\begin{aligned} \mathcal{L}_{\rho}(\lambda, \eta, e, d) = & - \sum_{i=1}^m \mu_i \lambda_i - \sum_{j=1}^n \nu_j \eta_j + \mathbb{I}_+(e) \\ & + \sum_{i=1}^m \sum_{j=1}^n d_{ij} (c_{ij} - \lambda_i - \eta_j - e_{ij}) + \frac{\rho}{2} \sum_{i=1}^m \sum_{j=1}^n (c_{ij} - \lambda_i - \eta_j - e_{ij})^2 \end{aligned} \quad (10)$$

The minimizer of e can be done directly by solving for zero gradient and projection, while the minimizer of λ and η can be done by solving for zero gradient.

$$\begin{aligned}
\operatorname{argmin}_{e_{ij}} \mathcal{L}_\rho(\lambda, \eta, e, d) &= \max \left(c_{ij} + \frac{d_{ij}}{\rho} - \lambda_i - \eta_j, 0 \right) \\
\operatorname{argmin}_{\lambda_i} \mathcal{L}_\rho(\lambda, \eta, e, d) &= \frac{1}{n} \left((\mu_i + \sum_{j=1}^n d_{ij}) / \rho + \sum_{j=1}^n (c_{ij} - \eta_j - e_{ij}) \right) \\
\operatorname{argmin}_{\eta_j} \mathcal{L}_\rho(\lambda, \eta, e, d) &= \frac{1}{m} \left((\nu_j + \sum_{i=1}^m d_{ij}) / \rho + \sum_{i=1}^m (c_{ij} - \lambda_i - e_{ij}) \right)
\end{aligned} \tag{11}$$

The algorithm is implemented in **ADMM_dual.py**. Solution π can be recovered by $\pi = -d$ from KKT conditions.

Algorithm 2: Alternating direction method of multipliers for the primal problem

Input: input data c, μ, ν , step size α , penalty scalar ρ and maximum iteration N

Output: solution π

```

1 initializing  $k = 0$ 
2  $\lambda^{(k)}, \eta^{(k)}, e^{(k)}, d^{(k)} := 0$ 
3 while  $k < N$  do
4    $\lambda_i^{(k+1)} := \operatorname{argmin}_{\lambda_i} \mathcal{L}_\rho(\lambda, \eta^{(k)}, e^{(k)}, d^{(k)})$ 
5    $\eta_j^{(k+1)} := \operatorname{argmin}_{\eta_j} \mathcal{L}_\rho(\lambda^{(k+1)}, \eta, e^{(k)}, d^{(k)})$ 
6    $e_{ij}^{(k+1)} := \operatorname{argmin}_{e_{ij}} \mathcal{L}_\rho(\lambda^{(k+1)}, \eta^{(k+1)}, e, d^{(k)})$ 
7    $d_{ij}^{(k+1)} := d_{ij}^{(k)} + \alpha \rho (c_{ij} - \lambda_i - \eta_j - e_{ij})$ 
8    $k := k + 1$ 
9 end
10 return  $\pi = -d$ 

```

3.3 Add Entropy Regularization: Sinkhorn-Knopp Algorithm

The discrete entropy of a coupling matrix is defined as [13]:

$$\mathbf{H}(\mathbf{P}) \stackrel{\text{def}}{=} - \sum_{i,j} \mathbf{P}_{i,j} (\log(\mathbf{P}_{i,j}) - 1) \tag{12}$$

The function \mathbf{H} is strongly concave, we can see it by computing its 2-order derivatives:

$$\frac{\partial^2 \mathbf{H}(\mathbf{P})}{\partial \mathbf{P}_{ij}^2} = -\operatorname{diag}(1/\mathbf{P}_{i,j}) \tag{13}$$

Notice that $\mathbf{P}_{i,j} \leq 1$, it's obvious that $\mathbf{H}(\mathbf{P})$ has a good property of convexity.

The idea of the entropic regularization of optimal transport is to use $-\mathbf{H}$ as a regularizing function to obtain approximate solutions to the original transport problem:

$$\mathbf{L}_C^\varepsilon(\mathbf{a}, \mathbf{b}) \stackrel{\text{def}}{=} \min_{\mathbf{P} \in \mathbf{U}(\mathbf{a}, \mathbf{b})} \langle \mathbf{P}, \mathbf{C} \rangle - \varepsilon \mathbf{H}(\mathbf{P}) \tag{14}$$

With strong convexity of $\mathbf{H}(\mathbf{P})$ our new target has a global minima.

For readers who are interest in its asymptotic property, we refer to [10]. Up to now, all we need to know is that we have

$$\lim_{\epsilon \rightarrow 0} L_C^\epsilon(\mathbf{a}, \mathbf{b}) = L_C(\mathbf{a}, \mathbf{b}) = \min_{\mathbf{P} \in \mathbf{U}(\mathbf{a}, \mathbf{b})} \langle \mathbf{P}, \mathbf{C} \rangle \quad (15)$$

What's more, this new target can be interpreted as $\text{KL}(\mathbf{P}|\mathbf{K})$:

$$\text{KL}(\mathbf{P}|\mathbf{K}) \stackrel{\text{def}}{=} \sum_{i,j} \mathbf{P}_{i,j} \log \left(\frac{\mathbf{P}_{i,j}}{\mathbf{K}_{i,j}} \right) - \mathbf{P}_{i,j} + \mathbf{K}_{i,j} \quad (16)$$

where \log is taken element-wise and $\mathbf{K}_{i,j} = e^{-\mathbf{C}_{i,j}/\epsilon}$, which will be interpreted later.

One can show that the solution to 14 has the form of

$$\mathbf{P}_{i,j} = \mathbf{u}_i \mathbf{K}_{i,j} \mathbf{v}_j \quad (17)$$

where $\mathbf{K}_{i,j} = e^{-\mathbf{C}_{i,j}/\epsilon}$ by calculating the KKT condition: Introducing two dual variables $\mathbf{f} \in \mathbb{R}^n, \mathbf{g} \in \mathbb{R}^n$ and calculate the lagrangian:

$$\mathcal{L}(\mathbf{P}, \mathbf{f}, \mathbf{g}) = \langle \mathbf{P}, \mathbf{C} \rangle - \epsilon \mathbf{H}(\mathbf{P}) - \langle \mathbf{f}, \mathbf{P} \mathbf{1}_n - \mathbf{a} \rangle - \langle \mathbf{g}, \mathbf{P}^T \mathbf{1}_n - \mathbf{b} \rangle \quad (18)$$

take first order gradient and we get

$$\frac{\partial \mathcal{L}(\mathbf{P}, \mathbf{f}, \mathbf{g})}{\partial \mathbf{P}_{i,j}} = \mathbf{C}_{i,j} + \epsilon \log(\mathbf{P}_{i,j}) - \mathbf{f}_i - \mathbf{g}_j = 0 \quad (19)$$

$$\Rightarrow \mathbf{P}_{i,j} = e^{\mathbf{f}_i/\epsilon} e^{-\mathbf{C}_{i,j}/\epsilon} e^{\mathbf{g}_j/\epsilon} \quad (20)$$

Thus we also get

$$\mathbf{u} = e^{\mathbf{f}/\epsilon} \quad (21)$$

$$\mathbf{v} = e^{\mathbf{g}/\epsilon} \quad (22)$$

Based on the constrain that:

$$\text{diag}(\mathbf{u}) \mathbf{K} \text{diag}(\mathbf{v}) \mathbf{1}_m = \mathbf{a} \quad (23)$$

$$\text{diag}(\mathbf{v}) \mathbf{K}^T \text{diag}(\mathbf{u}) \mathbf{1}_n = \mathbf{b} \quad (24)$$

or :

$$\mathbf{u} \odot (\mathbf{K} \mathbf{v}) = \mathbf{a} \quad \text{and} \quad \mathbf{v} \odot (\mathbf{K}^T \mathbf{u}) = \mathbf{b} \quad (25)$$

(where \odot means entry-wise multiplication of vectors) we can develop our algorithm as iteratively updating \mathbf{u} and \mathbf{v} , which is famous Sinkhorn-Knopp algorithm[12]:

$$\mathbf{u}^{(\ell+1)} = \frac{\mathbf{a}}{\mathbf{K} \mathbf{v}^{(\ell)}} \quad \text{and} \quad \mathbf{v}^{(\ell+1)} = \frac{\mathbf{b}}{\mathbf{K}^T \mathbf{u}^{(\ell+1)}} \quad (26)$$

with $\mathbf{v}^{(0)} = \mathbf{1}_m$ and $\mathbf{K}_{i,j} = e^{-\mathbf{C}_{i,j}/\epsilon}$.

The algorithm is implemented in **sinkhorn.py**. We remark that with different initial value for $\mathbf{v}^{(0)}$, the final solution for \mathbf{v} and \mathbf{u} would be different, since if we use $\lambda \mathbf{v}^{(0)}$

to replace \mathbf{v} , then we will get \mathbf{u}/λ at every iteration. Even so, our final solution for \mathbf{P} won't change based on the way we calculate it [20](#).

The effect of Sinkhorn-Knopp method is remarkable, the output (i.e. \mathbf{P}) evolves to a proper coupling for optimal transport³:

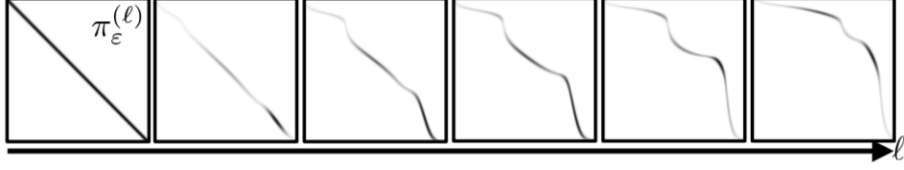


Figure 2: the development of \mathbf{P} w.r.t. iteration ℓ

3.4 Sinkhorn-Newton Method [11]

If we take $-\mathbf{f}, -\mathbf{g}$ to take place with \mathbf{f}, \mathbf{g} (notice that \mathbf{f}, \mathbf{g} are just multiplier for equality constrain, so changing their sign as a whole won't make any difference), then from [20](#) and [25](#) we can conclude that our target could be reformulated as finding a zero point of

$$F(\mathbf{f}, \mathbf{g}) := \begin{pmatrix} a - \text{diag}(e^{-\mathbf{f}/\epsilon}) \mathbf{K} e^{-\mathbf{g}/\epsilon} \\ b - \text{diag}(e^{-\mathbf{g}/\epsilon}) \mathbf{K}^T e^{-\mathbf{f}/\epsilon} \end{pmatrix}$$

where a, b, ϵ and \mathbf{K} are known. What we need to do is to use newton-raphson method to find its zero points [11]:

$$\begin{pmatrix} \mathbf{f}^{k+1} \\ \mathbf{g}^{k+1} \end{pmatrix} = \begin{pmatrix} \mathbf{f}^k \\ \mathbf{g}^k \end{pmatrix} - J_F(\mathbf{f}^k, \mathbf{g}^k)^{-1} F(\mathbf{f}^k, \mathbf{g}^k) \quad (27)$$

where the Jacobian of F is:

$$J_F(\mathbf{f}, \mathbf{g}) = \frac{1}{\epsilon} \begin{bmatrix} \text{Diag}(\mathbf{P} \mathbf{1}_m) & \mathbf{P} \\ \mathbf{P}^T & \text{Diag}(\mathbf{P}^T \mathbf{1}_n) \end{bmatrix} \quad (28)$$

that is, we can use conjugate gradient to solve

$$J_F(\mathbf{f}^k, \mathbf{g}^k) \begin{pmatrix} \delta \mathbf{f} \\ \delta \mathbf{g} \end{pmatrix} = -F(\mathbf{f}^k, \mathbf{g}^k) \quad (29)$$

and then update variables by

$$\begin{aligned} \mathbf{f}^{k+1} &= \mathbf{f}^k + \delta \mathbf{f} \\ \mathbf{g}^{k+1} &= \mathbf{g}^k + \delta \mathbf{g} \end{aligned} \quad (30)$$

Because $\mathbf{P}^k := \text{Diag}(e^{-\mathbf{f}^k/\epsilon}) \mathbf{K} \text{Diag}(e^{-\mathbf{g}^k/\epsilon})$, the update step can be rewrite as

$$\begin{aligned} \mathbf{P}^{k+1} &= \text{Diag}(e^{-[\mathbf{f}^k + \delta \mathbf{f}]/\epsilon}) \mathbf{K} \text{Diag}(e^{-[\mathbf{g}^k + \delta \mathbf{g}]/\epsilon}) \\ &= \text{Diag}(e^{-\delta \mathbf{f}/\epsilon}) \mathbf{P}^k \text{Diag}(e^{-\delta \mathbf{g}/\epsilon}) \end{aligned} \quad (31)$$

³figure taken from [13]

Algorithm 3: Sinkhorn-Newton method in primal variable

Input: $\mathbf{a} \in \Sigma_n, \mathbf{b} \in \Sigma_m, \mathbf{C} \in \mathbb{R}^{n \times m}$

- 1 initializing $\mathbf{P}^0 = \exp(-\mathbf{C}/\varepsilon)$, set $k = 0$
- 2 **repeat**
- 3 $\mathbf{a}^k \leftarrow \mathbf{P}^k \mathbf{1}_m$
- 4 $\mathbf{b}^k \leftarrow (\mathbf{P}^k)^\top \mathbf{1}_n$
- 5 compute $\delta \mathbf{f}, \delta \mathbf{g}$: $\frac{1}{\varepsilon} \begin{bmatrix} \text{Diag}(\mathbf{a}^k) & \mathbf{P}^k \\ (\mathbf{P}^k)^\top & \text{Diag}(\mathbf{b}^k) \end{bmatrix} \begin{bmatrix} \delta \mathbf{f} \\ \delta \mathbf{g} \end{bmatrix} = \begin{bmatrix} \mathbf{a}^k - \mathbf{a} \\ \mathbf{b}^k - \mathbf{b} \end{bmatrix}$
- 6 $\mathbf{P}^{k+1} \leftarrow \text{Diag}(e^{-\delta \mathbf{f}/\varepsilon}) \mathbf{P}^k \text{Diag}(e^{-\delta \mathbf{g}/\varepsilon})$
- 7 $k \leftarrow k + 1$
- 8 **until** *some stopping criteria fulfilled*;
- 9 return \mathbf{P}

The algorithm is implemented in `sinkhorn_newton.py`.

3.5 Sinkhorn-Newton for Dual Problem

For the dual problem

$$\mathcal{L}(\mathbf{P}, \mathbf{f}, \mathbf{g}) = \langle \mathbf{P}, \mathbf{C} \rangle - \varepsilon \mathbf{H}(\mathbf{P}) - \langle \mathbf{f}, \mathbf{P} \mathbf{1}_n - \mathbf{a} \rangle - \langle \mathbf{g}, \mathbf{P}^\top \mathbf{1}_m - \mathbf{b} \rangle \quad (32)$$

$$\frac{\partial \mathcal{L}(\mathbf{P}, \mathbf{f}, \mathbf{g})}{\partial \mathbf{P}_{i,j}} = 0 \quad (33)$$

$$\Rightarrow \hat{\mathbf{P}} = e^{\mathbf{f}/\varepsilon} e^{-\mathbf{C}/\varepsilon} e^{\mathbf{g}/\varepsilon} \quad (34)$$

$$\Rightarrow \mathcal{L}(\hat{\mathbf{P}}, \mathbf{f}, \mathbf{g}) = \langle \mathbf{f}, \mathbf{a} \rangle + \langle \mathbf{g}, \mathbf{b} \rangle - \varepsilon \langle e^{\mathbf{f}/\varepsilon}, \mathbf{K} e^{\mathbf{g}/\varepsilon} \rangle \quad (35)$$

We only need to solve

$$\max_{\mathbf{f} \in \mathbb{R}^n, \mathbf{g} \in \mathbb{R}^m} \langle \mathbf{f}, \mathbf{a} \rangle + \langle \mathbf{g}, \mathbf{b} \rangle - \varepsilon \langle e^{\mathbf{f}/\varepsilon}, \mathbf{K} e^{\mathbf{g}/\varepsilon} \rangle = Q(\mathbf{f}, \mathbf{g}) \quad (36)$$

(Notice that this is an approximation of the original Kantorovich dual

$$L_{\mathbf{C}}(\mathbf{a}, \mathbf{b}) = \max_{(\mathbf{f}, \mathbf{g}) \in \mathbf{R}(\mathbf{a}, \mathbf{b})} \langle \mathbf{f}, \mathbf{a} \rangle + \langle \mathbf{g}, \mathbf{b} \rangle \quad (37)$$

$$\mathbf{R}(\mathbf{a}, \mathbf{b}) \stackrel{\text{def}}{=} \{(\mathbf{f}, \mathbf{g}) \in \mathbb{R}^n \times \mathbb{R}^m : \forall (i, j) \in \mathbb{Z}[n] \times [m], \mathbf{f} \oplus \mathbf{g} \leq \mathbf{C}\} \quad (38)$$

)

We can calculate its gradient

$$\begin{aligned} \nabla|_{\mathbf{f}} Q(\mathbf{f}, \mathbf{g}) &= \mathbf{a} - e^{\mathbf{f}/\varepsilon} \odot (\mathbf{K} e^{\mathbf{g}/\varepsilon}) \\ \nabla|_{\mathbf{g}} Q(\mathbf{f}, \mathbf{g}) &= \mathbf{b} - e^{\mathbf{g}/\varepsilon} \odot (\mathbf{K}^T e^{\mathbf{f}/\varepsilon}) \end{aligned} \quad (39)$$

and its Hessian matrix respectively.

Then we derive the Newton-Raphson algorithm for minimizing $Q(\mathbf{f}, \mathbf{g})$:

Algorithm 4: Sinkhorn-Newton method in dual variable

Input: $\mathbf{a} \in \Sigma_n, \mathbf{b} \in \Sigma_m, \mathbf{K}$ and \mathbf{K}^\top

Output: solution \mathbf{P}

- 1 initializing $a^0 \in \mathbb{R}^n, b^0 \in \mathbb{R}^m$, set $k = 0$
 - 2 **repeat**
 - 3 $a^k \leftarrow e^{-f^k/\varepsilon} \odot K e^{-g^k/\varepsilon}$
 - 4 $b^k \leftarrow e^{-g^k/\varepsilon} \odot K^\top e^{-f^k/\varepsilon}$
 - 5 Compute updates δf and δg by solving $M \begin{bmatrix} \delta f \\ \delta g \end{bmatrix} = \begin{bmatrix} a^k - a \\ b^k - b \end{bmatrix}$
 - 6 where the application of M is given by
$$M \begin{bmatrix} \delta f \\ \delta g \end{bmatrix} = \frac{1}{\varepsilon} \begin{bmatrix} a^k \odot \delta f + e^{-f^k/\varepsilon} \odot K \left(e^{-g^k/\varepsilon} \odot \delta g \right) \\ b^k \odot \delta g + e^{-g^k/\varepsilon} \odot K^\top \left(e^{-f^k/\varepsilon} \odot \delta f \right) \end{bmatrix}$$
 - 7 $f^{k+1} \leftarrow f^k + \delta f$
 - 8 $g^{k+1} \leftarrow g^k + \delta g$
 - 9 $k \leftarrow k + 1$
 - 10 **until** *some stopping criteria fulfilled*;
 - 11 **return** \mathbf{P}
-

The algorithm is implemented in `sinkhorn_newton_dual.py`.

Or, in 39 we can set the gradient to 0 straightly

$$\mathbf{f}^{(\ell+1)} = \varepsilon \log \mathbf{a} - \varepsilon \log \left(\mathbf{K} e^{\mathbf{g}^{(\ell)}/\varepsilon} \right) \quad (40)$$

$$\mathbf{g}^{(\ell+1)} = \varepsilon \log \mathbf{b} - \varepsilon \log \left(\mathbf{K}^\top e^{\mathbf{f}^{(\ell+1)}/\varepsilon} \right) \quad (41)$$

for $\ell \geq 0$. However, it's actually the same as Sinkhorn-Knopp algorithm based on $(\mathbf{u}, \mathbf{v}) = (e^{\mathbf{f}/\varepsilon}, e^{\mathbf{g}/\varepsilon})$.

3.6 Log-domain Sinkhorn

[13] We can rewrite the above formula 40 and 41 as

$$\begin{aligned} \mathbf{f}^{(\ell+1)} &= \text{Min}_\varepsilon^{\text{row}} (\mathbf{S}(\mathbf{f}^{(\ell)}, \mathbf{g}^{(\ell)})) - \mathbf{f}^{(\ell)} + \varepsilon \log(\mathbf{a}) \\ \mathbf{g}^{(\ell+1)} &= \text{Min}_\varepsilon^{\text{col}} (\mathbf{S}(\mathbf{f}^{(\ell+1)}, \mathbf{g}^{(\ell)})) - \mathbf{g}^{(\ell)} + \varepsilon \log(\mathbf{b}) \end{aligned} \quad (42)$$

where $\mathbf{S}(\mathbf{f}, \mathbf{g}) = (\mathbf{C}_{i,j} - \mathbf{f}_i - \mathbf{g}_j)_{i,j}$ and

$$\begin{aligned} \text{Min}_\varepsilon^{\text{row}}(\mathbf{A}) &\stackrel{\text{def}}{=} \left(\min_\varepsilon (\mathbf{A}_{i,j})_j \right)_i \in \mathbb{R}^n \\ \text{Min}_\varepsilon^{\text{col}}(\mathbf{A}) &\stackrel{\text{def}}{=} \left(\min_\varepsilon (\mathbf{A}_{i,j})_i \right)_j \in \mathbb{R}^m \end{aligned} \quad (43)$$

and $\min_\varepsilon \mathbf{z} = -\varepsilon \log \sum_i e^{-\mathbf{z}_i/\varepsilon}$ for a vector \mathbf{z} . We implement this algorithm and name it as `sinkhorn_logdomain.py`.

Let's probe into this expression:

First, $\min_{\varepsilon} \mathbf{z}$ is nothing but a differentiable approximation of \min function. When we take $\varepsilon \rightarrow 0$, we have $\min_{\varepsilon} \mathbf{z} = \min \mathbf{z}$. Besides, the above formula 40 and 41 are just

$$(\mathbf{f}^{(\ell+1)})_i = \min_{\varepsilon} \left(\mathbf{C}_{ij} - \mathbf{g}_j^{(\ell)} \right)_j + \varepsilon \log \mathbf{a}_i \quad (44)$$

$$(\mathbf{g}^{(\ell+1)})_j = \min_{\varepsilon} \left(\mathbf{C}_{ij} - \mathbf{f}_i^{(\ell)} \right)_i + \varepsilon \log \mathbf{b}_j \quad (45)$$

where $\left(\mathbf{C}_{ij} - \mathbf{g}_j^{(\ell)} \right)_j$ denotes the soft-minimum of all values of the j -th column of matrix $\left(\mathbf{C} - \mathbf{1}_n (\mathbf{g}^{(\ell)})^T \right)$. If we define $\text{Min}_{\varepsilon}^{\text{row}}(\mathbf{A})$ and $\text{Min}_{\varepsilon}^{\text{col}}(\mathbf{A})$ as above, then we get

$$\mathbf{f}^{(\ell+1)} = \text{Min}_{\varepsilon}^{\text{row}} \left(\mathbf{C} - \mathbf{1}_n \mathbf{g}^{(\ell)T} \right) + \varepsilon \log \mathbf{a} \quad (46)$$

$$\mathbf{g}^{(\ell+1)} = \text{Min}_{\varepsilon}^{\text{col}} \left(\mathbf{C} - \mathbf{f}^{(\ell)} \mathbf{1}_m^T \right) + \varepsilon \log \mathbf{b} \quad (47)$$

After that we use a little stable trick

$$\min_{\varepsilon} \mathbf{z} = \underline{z} - \varepsilon \log \sum_i e^{-(\mathbf{z}_i - \underline{z})/\varepsilon} \quad (48)$$

where $\underline{z} = \min \mathbf{z}$. Instead of \underline{z} , we use former iteration's value $\mathbf{f}^{(\ell)}$, then we get 42.

3.7 More on Sinkhorn

Following [1] [2] [3] [4], the 14 could be think of as a special case of the following convex optimization problem

$$\min_{\mathbf{P}} \sum_{i,j} \mathbf{C}_{i,j} \mathbf{P}_{i,j} - \varepsilon \mathbf{H}(\mathbf{P}) + \iota_{\{\mathbf{a}\}}(\mathbf{P} \mathbf{1}_m) + \iota_{\{\mathbf{b}\}}(\mathbf{P}^T \mathbf{1}_n) \quad (49)$$

where ι_C means the indicator of set C , which is

$$\iota_C(x) = \begin{cases} 0 & \text{if } x \in C \\ +\infty & \text{otherwise} \end{cases} \quad (50)$$

Under this situation, the Sinkhorn-Knopp iteration can be extended as

$$\mathbf{u} \leftarrow \frac{\text{Prox}_F^{\text{KL}}(\mathbf{K} \mathbf{v})}{\mathbf{K} \mathbf{v}} \quad (51)$$

$$\mathbf{v} \leftarrow \frac{\text{Prox}_G^{\text{KL}}(\mathbf{K}^T \mathbf{u})}{\mathbf{K}^T \mathbf{u}} \quad (52)$$

where the proximal operator for KL divergence is defined as

$$\text{Prox}_F^{\text{KL}}(\mathbf{u}) = \underset{\mathbf{u}' \in \mathbb{R}_+^N}{\text{argmin}} \text{KL}(\mathbf{u}' | \mathbf{u}) + F(\mathbf{u}'), \forall \mathbf{u} \in \mathbb{R}_+^N \quad (53)$$

(an extention of normal proximal operator)

4 Numerical Result and Interpretation

4.1 Description of Datasets

In order to compare the performance of different algorithms, we have to use some classic and challenging datasets.

In general, the i -th datapoint can be denoted as (x_i, μ_i) , where $x_i \in \mathbb{R}^d$ is the position of datapoint and μ_i is the probability at x_i .

For convenience, we assume that datapoints are followed 2D distribution (i.e. $x_i \in \mathbb{R}^2$). Besides, we use the squared Euclidean distance to define the cost matrix between two datas $\{(x_i, \mu_i)\}_{i=1}^m$ and $\{(y_j, \nu_j)\}_{j=1}^n$ as following

$$c_{ij} = \|x_i - y_j\|_2^2 \quad \forall i, j \quad (54)$$

We have tested our algorithms on four types of datasets

- Randomly generated dataset

The position are uniformly sampled from $[0, 1] \times [0, 1]$. The weights μ and ν are randomly sampled from $[0, 1]$ and scaled to $\sum_{i=1}^m \mu_i = \sum_{j=1}^n \nu_j = 1$.

- ellipses [Gerber2017]

The ellipse example consists of two uniform samples (source and target data set) of size $m = n$ from the unit circle with normal distributed noise added with zero mean and standard deviation 0.1. The source data sample is then scaled in the x-Axis by 0.5 and in the y-Axis by 2, while the target data set is scaled in the x-Axis by 2 and in the y-Axis by 0.5. Besides, the weights are both normalized uniform distributions.

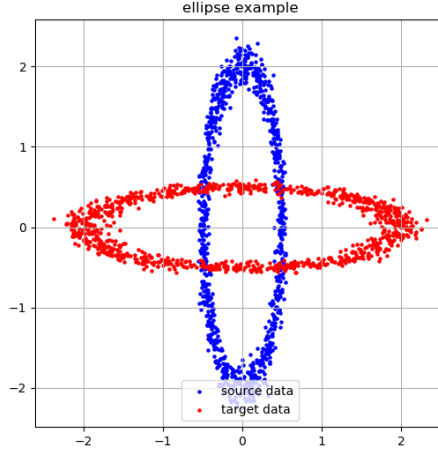


Figure 3: $m = n = 1000$, ellipse example

- Caffarelli [Gerber2017]

Caffarelli's example consists of two uniform samples (source and target data

set) on $[-1, 1] \times [-1, 1]$ of size $m = n$. Any points outside the unit circle are then discarded. Additionally, the target data sample is split along the x-Axis at 0 and shifted by $+2$ and -2 for points with positive and negative x-Axis values, respectively. The weights are both normalized uniform distributions, too.

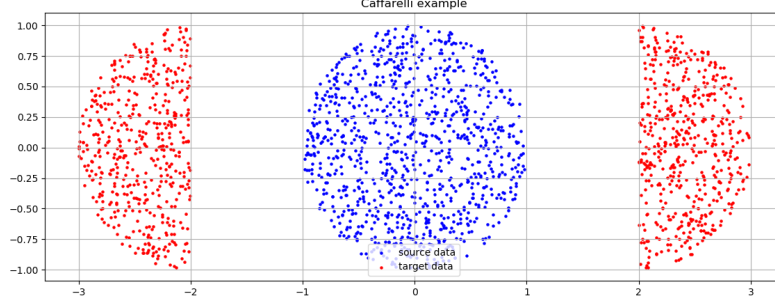


Figure 4: $m = n = 1000$, Caffarelli's example

- DOTmark [Schrieber2017]

In DOTmark, we always have $m = n = r^2$, and $(x_i)_{1 \leq i \leq m} = (y_j)_{1 \leq j \leq n}$ form a regular square grid of resolution $r \times r$ in \mathbb{R}^2 , which are the natural position of source and target data set. The weights are the brightness distributions with normalization. Besides, DOTmark consists of 10 classes of 10 different images, each of which is available at the 5 different resolutions from 32×32 to 512×512 (in doubling steps per dimension).

#	Name
1	WhiteNoise
2	GRFrough
3	GRFmoderate
4	GRFsmooth
5	LogGRF
6	LogitGRF
7	CauchyDensity
8	Shapes
9	ClassicImages
10	Microscopy

Table 1: The 10 classes in the DOTmark

4.2 Numerical Result

In this section, we will show the performance of different algorithms or solvers for the above mentioned datasets. For convenience, MOSEK and Gurobi are denoted by **M** and **G** respectively. Besides, 'prim', 'dual' and 'int' are corresponding to 'primal simplex', 'dual simplex' and 'interior point'.

In order to evaluate the performance of different algorithms and solvers, we mark down some experimental performance indicators. '**dist**' stands for the Wasserstein distance, which equals $\sum_i \sum_j c_{ij} \pi_{ij}$ for discrete optimal transport. '**time**' stands for the using time for solving OT problem. Besides, we set the fixed iterations=15000 for ADMM primal, 3000 for sinkhorn and 30 for sinkhorn-Newton in the whole numerical experiment. What's more, we also took the errors of weight into consideration via 2 indicators '**err μ** ' and '**err ν** '.

$$\begin{aligned} err\mu &= \sum_{i=1}^m \left| \sum_{j=1}^n \pi_{ij} - \mu_i \right| \\ err\nu &= \sum_{j=1}^n \left| \sum_{i=1}^m \pi_{ij} - \nu_j \right| \end{aligned} \quad (55)$$

In order to make a comprehensive comparison between different algorithms and solvers, we had tested 4 different scale, $m = n = 256, 512, 1024, 2048$ when used random, ellipse and Caffarelli dataset.

$m = n$		M prim	M dual	M int	G prim	G dual	G int	ADMM primal	Sinkhorn
256	dist	5.45e-3	7.25e-3	8.09e-3	5.94e-3	8.62e-3	5.13e-3	5.04e-3	8.64e-3
	time	3.43e-1	3.75e-1	5.28e-1	6.79e-1	7.07e-1	8.56e-1	26.82	4.19
	err μ	1.79e-5	2.04e-17	2.31e-12	1.34e-17	9.97e-18	4.34e-18	4.67e-5	7.01e-3
	err ν	1.79e-5	2.45e-16	2.79e-12	5.36e-16	3.87e-16	5.05e-16	4.74e-5	8.54e-17
512	dist	2.90e-3	2.88e-3	3.37e-3	3.79e-3	2.91e-3	5.52e-3	3.13e-3	3.61e-3
	time	1.39	1.70	2.93	2.83	3.40	4.27	1.03e+2	25.8
	err μ	4.35e-5	2.67e-17	1.30e-13	1.08e-17	1.09e-15	1.21e-17	8.40e-5	8.65e-3
	err ν	4.35e-5	1.09e-16	1.04e-13	1.72e-16	1.26e-17	7.46e-16	8.39e-5	1.20e-16
1024	dist	1.78e-3	1.94e-3	1.89e-3	1.91e-3	1.80e-3	1.84e-3	2.94e-3	2.79e-3
	time	8.11	15.3	15.2	14.1	14.0	18.7	4.52e+2	1.53e+2
	err μ	1.04e-4	1.09e-16	1.38e-12	1.01e-17	1.12e-17	1.91e-15	2.27e-4	1.07e-2
	err ν	1.04e-4	1.91e-15	1.27e-12	6.49e-16	3.42e-16	9.43e-18	2.20e-4	1.18e-16
2048	dist	1.35e-3	1.36e-3	1.31e-3	1.42e-3	1.46e-3	1.49e-3	1.48e-3	1.06e-3
	time	35.0	1.05e+2	68.7	3.45e+2	58.4	88.9	8.74e+3	1.99e+3
	err μ	2.71e-4	2.61e-16	1.81e-12	9.41e-18	6.09e-16	4.95e-16	8.99e-4	3.93e-3
	err ν	2.7e-4	1.79e-15	2.27e-12	1.27e-15	1.17e-17	1.13e-17	8.40e-4	1.48e-16

Table 2: Numerical result of random dataset

$m = n$		M prim	M dual	M int	G prim	G dual	G int	ADMM primal	Sinkhorn
256	dist	2.37	2.27	1.88	2.28	2.12	2.26	2.22	2.419
	time	5.42e-1	9.80	4.10	6.57e-1	1.49	7.22e-1	37.5	20.8
	err μ	1.76e-5	9.54e-18	1.65e-12	0	0	0	1.42e-5	6.98e-17
	err ν	1.76e-5	9.54e-18	1.65e-12	0	0	0	1.40e-5	4.54e-16
512	dist	2.36	2.39	2.24	2.15	2.31	2.32	2.47	2.38
	time	1.65	5.01	1.49	4.87	4.62	4.01	2.48e+2	72.2
	err μ	4.05e-5	2.04e-17	2.01e-11	0	0	0	3.39e-5	1.05e-16
	err ν	4.05e-5	1.95e-17	2.01e-11	0	0	0	3.40e-5	6.26e-16
1024	dist	2.24	2.11	2.21	2.24	2.18	2.27	2.25	2.39
	time	7.89	70.4	9.73	64.5	21.9	16.6	8.41e+2	2.68e+2
	err μ	9.39e-5	1.59e-16	5.37e-10	0	0	0	1.02e-4	1.25e-16
	err ν	9.39e-5	1.48e-16	5.37e-10	0	0	0	1.02e-4	6.47e-16
2048	dist	2.38	2.23	2.28	2.27	2.22	2.37	2.31	2.27
	time	32.6	4.37e+2	47.9	1.16e+3	8.24e+2	81.9	7.88e+3	6.52e+3
	err μ	2.42e-4	1.29e-16	1.52e-13	0	0	0	4.67e-3	1.21e-15
	err ν	2.42e-4	1.31e-16	1.40e-13	0	0	0	4.65e-3	1.07e-15

Table 3: Numerical result of ellipse example

$m = n$		M prim	M dual	M int	G prim	G dual	G int	ADMM primal	Sinkhorn
256	dist	4.06	3.91	4.03	4.08	3.86	4.15	4.02	4.24
	time	2.82e-1	8.80	6.54e-1	6.80e-1	1.96	7.63e-1	55.2	12.4
	err μ	1.67e-5	2.78e-17	1.98e-12	0	0	0	4.07e-6	6.46e-17
	err ν	1.67e-5	2.78e-17	1.98e-12	0	0	0	4.03e-6	4.59e-16
512	dist	3.95	3.97	4.05	4.10	3.97	3.96	3.99	4.21
	time	1.88	5.37	3.60	3.50	3.61	4.63	4.00e+2	50.3
	err μ	4.14e-5	7.55e-17	5.79e-12	0	0	0	4.03e-5	9.84e-17
	err ν	4.14e-5	7.59e-17	5.79e-12	0	0	0	4.08e-5	6.09e-16
1024	dist	3.99	4.04	4.09	4.00	4.00	3.95	3.97	4.35
	time	6.01	49.9	14.8	29.9	18.7	22.8	1.52e+3	1.72e+2
	err μ	9.80e-5	1.40e-16	8.04e-12	0	0	0	4.42e-4	1.33e-16
	err ν	9.80e-5	1.40e-16	8.12e-12	0	0	0	4.43e-4	6.29e-16
2048	dist	3.97	3.99	4.06	3.99	3.97	4.00	4.04	4.13
	time	27.9	4.93e+2	58.0	7.47e+2	1.02e+2	1.02e+1	1.06e+4	8.44e+3
	err μ	2.54e-4	3.95e-16	2.53e-13	0	0	0	8.60e-3	1.83e-16
	err ν	2.54e-4	3.96e-16	2.49e-13	0	0	0	8.60e-3	9.74e-16

Table 4: Numerical result of Caffarelli's example

Due to the limited time, we only tested a randomly chosen pair of images from each class with size 32×32 , whose corresponding cost matrix is 1024×1024 .

For solvers, it seems that Gurobi may always reach the truly optimal solution, while MOSEK sometimes fails and result in large errors of weight. For MOSEK, the primal simplex method are faster than the interior method and the dual simplex method, but larger errors of weight. For Gurobi, simplex methods are generally faster than interior point methods, because an simplex methods are specified for linear programs. The bad performance of the dual simplex may result from the huge

#		M prim	M dual	M int	G prim	G dual	G int	ADMM primal	Sinkhorn
1	dist	6.93e-4	6.93e-4	6.93e-4	6.93e-4	6.93e-4	6.93e-4	6.92e-4	6.62e-4
	time	9.50	10.0	11.9	15.6	11.3	1.73e+2	1.46e+3	1.49e+2
	err μ	1.02e-4	1.59e-16	3.39e-12	0	0	0	1.01e-4	7.90e-3
	err ν	1.02e-4	1.19e-9	1.20e-9	1.19e-9	1.19e-9	1.19e-9	1.01e-4	6.63e-17
2	dist	1.44e-3	1.44e-3	1.44e-3	1.44e-3	1.44e-3	1.44e-3	1.44e-3	1.27e-3
	time	7.34	15.7	10.3	14.4	14.4	26.5	1.59e+3	1.51e+2
	err μ	9.91e-5	1.10e-16	6.47e-13	0	0	2.58e-9	1.72e-4	1.15e-2
	err ν	9.91e-5	2.58e-9	2.58e-9	2.58e-9	2.58e-9	0	1.68e-4	1.29e-16
3	dist	3.98e-3	3.98e-3	3.98e-3	3.98e-3	3.98e-3	3.98e-3	3.98e-3	3.99e-3
	time	5.55	20.4	10.5	13.64	13.2	18.49	1.48e+3	1.52e+2
	err μ	9.84e-5	1.89e-16	7.38e-14	0	5.70e-10	0	1.16e-4	1.12e-3
	err ν	9.84e-5	5.70e-10	5.70e-10	5.70e-10	0	0	1.63e-4	1.82e-16
4	dist	2.09e-2	2.09e-2	2.09e-2	2.09e-2	2.09e-2	2.09e-2	2.09e-2	2.20e-2
	time	5.56	31.8	9.55	13.9	15.9	22.1	1.44e+3	1.25e+2
	err μ	9.78e-5	1.67e-16	9.80e-12	0	0	0	1.65e-4	1.23e-9
	err ν	9.78e-5	9.89e-8	1.24e-9	1.23e-9	1.23e-9	1.23e-9	1.63e-4	3.40e-16
5	dist	1.87e-2	1.87e-2	1.87e-2	1.87e-2	1.87e-2	1.87e-2	1.87e-2	1.97e-2
	time	5.99	20.4	10.3	14.2	16.8	29.4	1.54e+3	1.32e+2
	err μ	1.00e-4	1.55e-16	2.93e-12	0	0	0	1.16e-4	1.70e-9
	err ν	1.00e-4	1.59e-9	1.59e-9	1.59e-9	8.56e-10	1.59e-9	1.35e-4	3.07e-16
6	dist	1.65e-2	1.65e-2	1.65e-2	1.65e-2	1.65e-2	1.65e-2	1.65e-2	1.74e-2
	time	6.43	18.1	13.7	13.4	16.8	19.1	1.42e+3	1.31e+2
	err μ	1.00e-4	1.80e-16	4.20e-10	0	0	0	1.17e-4	4.11e-8
	err ν	1.00e-4	8.56e-10	1.28e-9	1.16e-9	8.56e-10	8.56e-10	1.20e-4	2.74e-16
7	dist	1.71e-2	1.71e-2	1.71e-2	1.71e-2	1.71e-2	1.71e	1.71e-2	1.80e-2
	time	8.66	29.7	12.5	13.4	18.0	26.4	1.54e+3	91.3
	err μ	1.09e-4	1.19e-16	4.09e-10	0	0	0	5.64e-4	1.16e-9
	err ν	1.09e-4	1.16e-9	1.57e-9	1.16e-9	1.16e-9	1.16e-9	4.35e-4	2.89e-16
8	dist	2.38e-2	2.38e-2	2.38e-2	2.38e-2	2.38e-2	2.38e-2	2.38e-2	2.50e-2
	time	5.17	6.84	6.33	13.3	12.2	12.2	1.56e+3	1.41e+2
	err μ	6.52e-5	1.17e-16	4.72e-11	0	0	0	8.20e-4	2.24e-8
	err ν	6.53e-5	2.24e-8	2.25e-8	2.24e-8	2.24e-8	2.24e-8	2.94e-4	4.48e-16
9	dist	6.12e-3	6.12e-3	6.12e-3	6.12e-3	6.12e-3	6.12e-3	6.13e-3	6.20e-3
	time	5.71	17.56	12.9	15.1	13.2	18.4	1.62e+3	1.51e+2
	err μ	9.90e-5	1.61e-16	9.08e-13	0	2.18e-11	0	1.16e-4	2.18e-11
	err ν	9.90e-5	2.18e-11	2.26e-11	2.18e-11	0	2.18e-11	1.21e-4	5.55e-16
10	dist	1.06e-2	1.06e-2	1.06e-2	1.06e-2	1.06e-2	1.06e-2	1.06e-2	1.09e-2
	time	4.20	7.32	6.00	12.8	13.9	20.9	1.71e+3	1.51e+2
	err μ	7.01e-5	1.16e-16	2.40e-11	0	0	5.94e-9	1.20e-4	1.23e-6
	err ν	7.01e-5	5.94e-9	5.95e-9	5.94e-9	5.94e-9	0	1.76e-4	2.24e-16

Table 5: Numerical result of 10 classes in the DOTmark

amount of constraints. Gurobi being generally better than MOSEK because of defect of the Python interface of MOSEK.

From the overall numerical results, we found that all the algorithms converge, but there are still some difference. As a stable and universal algorithm, the performance of ADMM primal is not completely capable of different problems. ADMM primal needs thousands of iterations to reach optimal value, but errors of weight needs more

iterations to reach $1e-4$ or fewer. Thus, the using time of ADMM primal is the worst one.

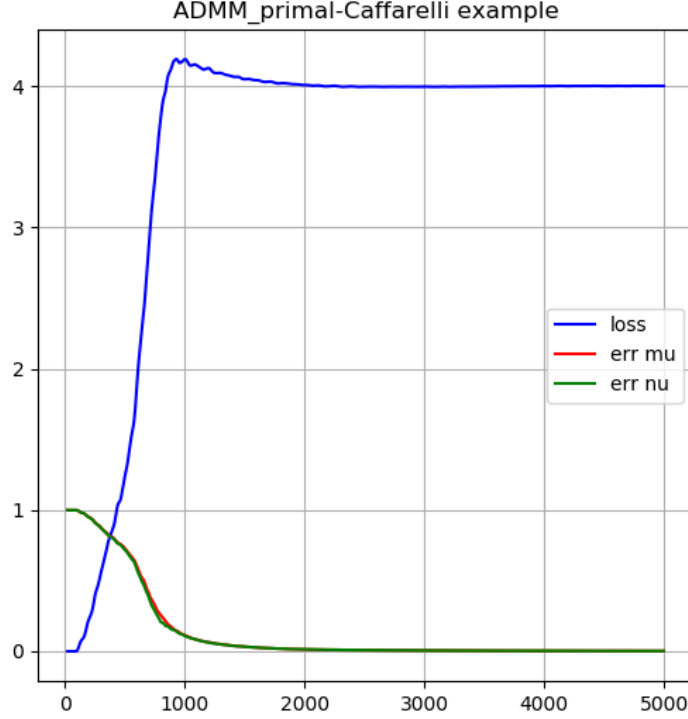


Figure 5: $m = n = 1000$, solving Caffarelli's example via ADMM primal

The implementation and thinking of Sinkhorn algorithm are nothing difficult. The number of hyperparameter is only one, ϵ . From the above mentioned theoretical introduction of Sinkhorn, ϵ stands for the weight of entropy regularization. If ϵ is extremely large, the entropy term will be the dominant of the problem, which will mislead the original problem to a completely different problem. Thus, the optimal solution of this problem will larger than true optimal value. On the other hand, If ϵ is extremely small, the entropy term can be ignored and makes no difference in this problem. In particular experiment, when using extremely small ϵ , the algorithm will be unstable and always overflow due to the defect of float point.

All the codes are implemented in Python.

4.3 A Discussion of Sinkhorn-Newton Algorithm

Comparing with sinkhorn algorithm, we can easily find that the using time of sinkhorn-Newton are longer than sinkhorn at small-scale datasets. Because, sinkhorn-Newton algorithm has an expensive step to solve a linear equation. However, when solving large-scale datasets, the efficiency of sinkhorn-Newton is better than

sinkhorn due to fewer iterations. For sinkhorn algorithm, it usually needs hundreds of iterations in order to decrease $\text{err } \mu$, while sinkhorn-Newton algorithm only needs dozens of iterations. Besides, sinkhorn-Newton algorithm has great performance of $\text{err } \mu$ and $\text{err } \nu$, even better than Gurobi and MOSEK.

$m = n$		random	ellipse	Caffarelli
256	dist	9.70e-3	2.59	4.53
	time	14.4	23.9	11.0
	$\text{err } \mu$	8.82e-15	3.01e-15	2.68e-16
	$\text{err } \nu$	1.47e-14	3.53e-15	3.21e-16
512	dist	6.22e-3	2.48	4.23
	time	67.7	95.4	80.5
	$\text{err } \mu$	8.75e-16	6.15e-16	1.43e-15
	$\text{err } \nu$	1.24e-15	7.05e-16	1.53e-15
1024	dist	5.4e-3	2.49	4.28
	time	1.69e+2	2.83e+2	2.52e+2
	$\text{err } \mu$	1.72e-14	2.02e-16	1.25e-16
	$\text{err } \nu$	2.15e-14	5.96e-16	6.28e-16
2048	dist	4.36e-3	2.50	4.28
	time	1.22e+3	1.18e+3	1.23e+3
	$\text{err } \mu$	1.88e-14	2.23e-16	1.90e-16
	$\text{err } \nu$	2.39e-14	8.64e-16	8.59e-16

Table 6: Numerical result of Sinkhorn-Newton algorithm

However, sinkhorn-Newton algorithm isn't a stable and universal algorithm. The value of hyperparameter ϵ is extremely sensitive towards different datasets. From the simplification of algorithm, we can find that ϵ only makes a difference at the initial step to smooth cost matrix c . In this way, if ϵ is extremely large, the cost matrix will close to zero matrix, which smooths over the characteristics of different cost matrix and results in bigger distance between two datas than Wasserstein distance. On the other hand, if ϵ is lower than specific critical value, the singularity of cost matrix will be strengthened via exponential function, which results in the Instability of solving linear equation and finally overflowing.

4.4 A Discussion of Sinkhorn-Newton Dual Algorithm

What's embarrassing is that we don't make it to find a proper parameter for Sinkhorn-Newton dual algorithm. What's more, strange things happens as the final loss (distance) output is always higher than the true distance (mosek/gurobi output) although the dual method achieves similar error results as its primal opponent and a faster performance. A possible explanation is that there may be a small dual gap due to the entropy regularization term introduced in by us, and it is enlarged by our mistakes at improper numerical process such as conjugate gradient.

$m = n$		random	ellipse	Caffarelli
256	dist	0.27	3.93	6.12
	time	5.14	7.54	10.3
	err μ	4.57e-15	3.32e-16	8.45e-16
	err ν	9.45e-15	5.13e-16	2.89e-16
512	dist	0.32	4.48	6.02
	time	10.52	11.98	20.4
	err μ	4.50e-15	3.75e-16	3.47e-16
	err ν	3.58e-16	7.48e-16	8.01e-16
1024	dist	0.33	4.19	6.28
	time	90.27	1.83e+2	2.12e+2
	err μ	4.85e-14	3.12e-16	2.34e-16
	err ν	6.32e-14	4.87e-16	4.92e-16
2048	dist	0.30	4.30	6.78
	time		8.8e+2	1.23e+3
	err μ	3.98e-14	4.98e-16	7.34e-16
	err ν	9.45e-14	5.70e-16	5.28e-16

Table 7: Numerical result of Sinkhorn-Newton Dual algorithm

4.5 The Changing Process of \mathbf{P} : the Merit of Sinkhorn-Newton Algorithm

For optimal transport problem between two one-dimensional distributions, we can easily see the connection between them and their final coupling \mathbf{P} as in 1. Besides we can visualize the changing process of \mathbf{P} and get a clear view of how the algorithm help to find the optimal transport. However, for two-dimensional distributions, there is a gap of it because we priory reshape a two-dimensional distribution into one-dimension to apply our algorithm and lose the visualizability.

Still, the change of coupling \mathbf{P} can give us some insights of different algorithms. First let's see that of ADMM_primal:

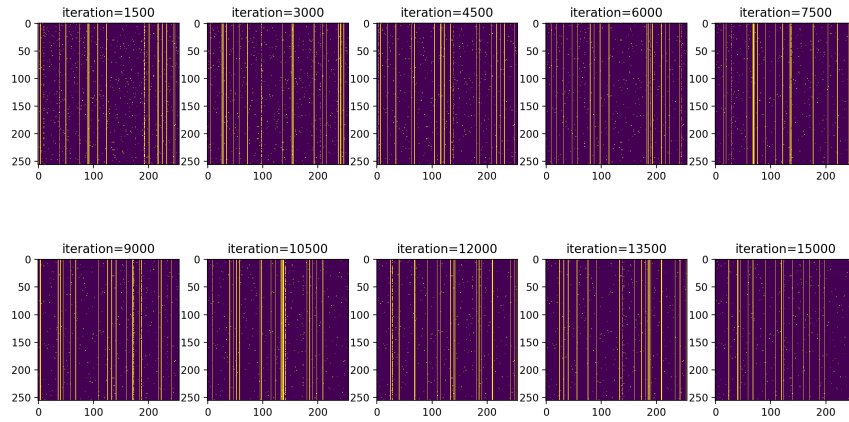


Figure 6: \mathbf{P} 's change of ADMM primal

Here we choose the ellipse dataset. It's astonishing that the plot result shows in one direction, the vertical direction, the \mathbf{P} is exactly uniformly equal. Even if we turn to other datasets, ADMM remains this, indicating this kind of change is a property of algorithm.

How about Sinkhorn?

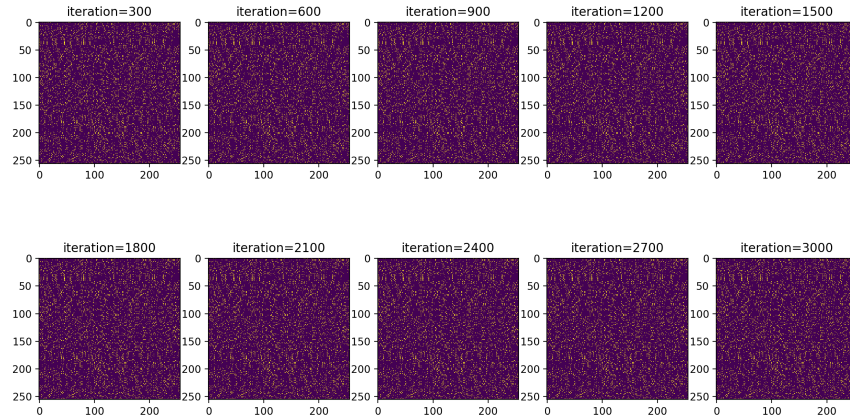


Figure 7: \mathbf{P} 's change of Sinkhorn

It seems totally random. Finally, let's see Sinkhorn-Newton:

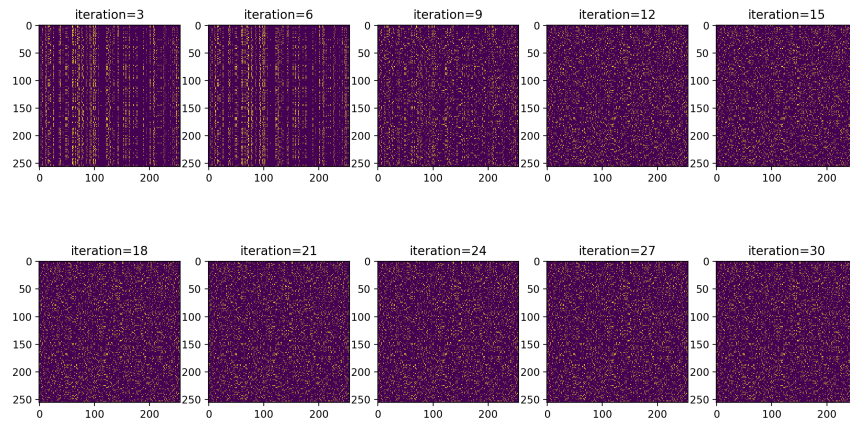


Figure 8: \mathbf{P} 's change of Sinkhorn-Newton

We find that at the early stage, Sinkhorn-Newton algorithm behaves just like ADMM primal and then it turns into a Sinkhorn-like one. It converges fast at an early age

with the aid of ADMM-like property and then get to a stable solution with Sinkhorn’s solution property. According to this explanation, though it’s somewhat heuristic, we can now say that the Sinkhorn-Newton is an algorithm that combines the merits of ADMM and Sinkhorn.

5 Conclusion and More

We have tried several first-order and second-order methods which have good performance in the context of discrete optimal transport, including ADMM-based methods and Entropy regularization-based methods, and both have their own merits and drawbacks. We run thorough experiments to test their performances and make comprehensive comparisons in many aspects in [4](#).

As for our next move, we aim to refine some of our existing algorithms to have a more stable performance and higher convergence rate. For some of our algorithms, we find some empirical tuning skills and we will consider their inner relationships with the iteration process. We also have ambition to test multi-stage iteration step on dual of ADMM and other methods, holding the believe that on different scale we need to provide different parameters.

Due to the limited time and equipment, we don’t test our algorithms at all scale of DOTmark dataset. At larger scale, there may be a need for different methods, which is to be explored by us.

Acknowledgments

We would like to thank Zhihan Li, Haochen Gan and Jason Jia for their useful instruction.

References

- [1] Karlsson, J., & Ringh, A. (2017). Generalized Sinkhorn iterations for regularizing inverse problems using optimal mass transport. *SIAM Journal on Imaging Sciences*, 10(4), 1935-1962.
- [2] Peyré, G. (2015). Entropic approximation of Wasserstein gradient flows. *SIAM Journal on Imaging Sciences*, 8(4), 2323-2351.
- [3] Frogner, C., Zhang, C., Mobahi, H., Araya, M., & Poggio, T. A. (2015). Learning with a Wasserstein loss. In *Advances in Neural Information Processing Systems* (pp. 2053-2061).
- [4] Chizat, L., Peyré, G., Schmitzer, B., & Vialard, F. X. (2016). Scaling algorithms for unbalanced transport problems. *arXiv preprint arXiv:1607.05816*.
- [5] L. Ambrosio. Lecture notes on optimal transport problems. In *Mathematical Aspects of Evolving Interfaces*, volume 1812 of *Lecture Notes in Mathematics*, pages 1–52. Springer, 2003
- [6] Bertsekas, D. P. (1992). Auction algorithms for network flow problems: A tutorial introduction. *Computational optimization and applications*, 1(1), 7-66.
- [7] Schrieber, J., Schuhmacher, D., & Gottschlich, C. (2017). Dotmark—a benchmark for discrete optimal transport. *IEEE Access*, 5, 271-282.
- [8] Villani, C. (2008). *Optimal transport: old and new* (Vol. 338). Springer Science & Business Media.

- [9] Gerber, S., & Maggioni, M. (2017). Multiscale strategies for computing optimal transport. *The Journal of Machine Learning Research*, 18(1), 2440-2471.
- [10] Cominetti, R., & San Martín, J. (1994). Asymptotic analysis of the exponential penalty trajectory in linear programming. *Mathematical Programming*, 67(1-3), 169-187.
- [11] Brauer, C., Clason, C., Lorenz, D., & Wirth, B. (2017). A Sinkhorn-Newton method for entropic optimal transport. *arXiv preprint arXiv:1710.06635*.
- [12] Sinkhorn, R., & Knopp, P. (1967). Concerning nonnegative matrices and doubly stochastic matrices. *Pacific Journal of Mathematics*, 21(2), 343-348.
- [13] Peyré, G., & Cuturi, M. (2017). Computational optimal transport (No. 2017-86).